JMES The International Journal of
Mechanical Engineering and Sciences
https://journal.its.ac.id/index.php/jmes/index
e-ISSN 2580-7471

Reducing Pressure Loss in Circulating Fluidized Bed Boiler: A Comparative Study of Innovative and Conventional Bell-Type Air-Caps

Hafid Alwan[1*], Anton Irawan[1], Yazid Bindar[2], Dwi Zacky Al Khoisi[1], Mochamad Naufal Alawiansyah[1], Oppy Oktaviani Pajri[1], Syifa Ainun Mauk[1]

[1]Department of Chemical Engineering, University of Sultan Ageng Tirtayasa, Jalan Jenderal Sudirman Km. 3, Cilegon 42435, Indonesia

[2]Department of Chemical Engineering, Faculty of Industrial Technology, Institut Teknologi Bandung, Jalan Ganesha 10, Bandung 40132, Indonesia

Received: 28 June 2026 , Revised: 7 July 2026, Accepted: 27 July 2026

Abstract

Pressure loss across the primary-air distributor influences the hydrodynamic performance of circulating fluidized-bed (CFB) systems. This study experimentally compared conventional and innovative bell-type air-caps based on their pressure-drop responses and bed behavior under cold-flow conditions. Experiments were conducted in a rectangular fluidization column using silica sand and low-rank coal at initial bed heights of 30 and 40 cm and superficial gas velocities of 7.94–38.25 cm/s. The apparent minimum fluidization velocity (U_{mf}) of silica sand was identified from the transition in the pressure-drop–velocity (ΔP–U) curve, supported by the observed bed expansion, and was approximately 30.67 cm/s at both bed heights. Low-rank coal exhibited only localized particle movement at higher gas velocities; no stable pressure-drop plateau or full-bed fluidization was observed within the tested velocity range. At U_{mf}, the innovative bell-type air-cap reduced the measured pressure loss by 11.9–16.6% across the four pressure-drop measurement locations (ΔP_1–ΔP_4) relative to the conventional design. This reduction indicates lower flow resistance and suggests the potential to reduce the pressure requirement of the air-supply system, although airflow uniformity and energy savings were not measured directly. The Wen–Yu correlation provided the closest prediction of U_{mf}, with a relative error of 12.7%, whereas the Basu and Ergun-based calculations produced errors of 33.4% and 80.1%, respectively. These results demonstrate that air-cap geometry affects pressure loss, while the accuracy of theoretical correlations depends strongly on particle and bed characteristics.

Keywords: Fluidized Bed, Air-cap, Bell-type, Air Distribution, Pressure Drop.

1. Introduction

Circulating fluidized-bed (CFB) boilers are widely applied in energy-conversion systems because of their fuel flexibility, effective gas–solid mixing, and relatively high combustion efficiency. Their hydrodynamic performance is strongly influenced by the distribution of primary air at the distributor level. Inadequate air distribution can promote channeling, localized pressure gradients, poor gas–solid contact, and unstable bed behavior, which may subsequently impair combustion performance and increase pollutant formation [1,2]. Therefore, air-cap geometry is an important design parameter because it affects the pressure drop (ΔP), gas delivery into the particle bed, and stability of the transition from the fixed-bed to the fluidized-bed regime.

Previous studies have investigated various air-distributor and bell-type air-cap configurations using numerical simulations and experimental methods [1–3]. However, direct experimental comparisons of conventional (Figure 1(a)) and modified bell-type air-caps under identical cold-flow conditions (Figure 1(b)) remain limited, particularly when bed materials with distinctly different particle sizes, densities, and fluidization characteristics are considered. Consequently, additional experimental evidence is required to clarify how air-cap geometry affects pressure loss and bed behavior for Geldart B silica sand and Geldart D low-rank coal.

This research hypothesizes that the innovative bell-type air-cap produces a lower pressure loss and a more even hydrodynamic response than the conventional design. Its modified internal passage and outlet configuration are expected to reduce contraction and turning losses and to alter the way gas is discharged into the particle bed. Because local gas-velocity profiles and nozzle-jet penetration were not measured directly, the performance of the two designs was evaluated using the measured pressure-drop responses at four pressure-tapping locations, observed bed

*Corresponding author. Email: hafidalwan@untirta.ac.id, phone: +62 85716560027

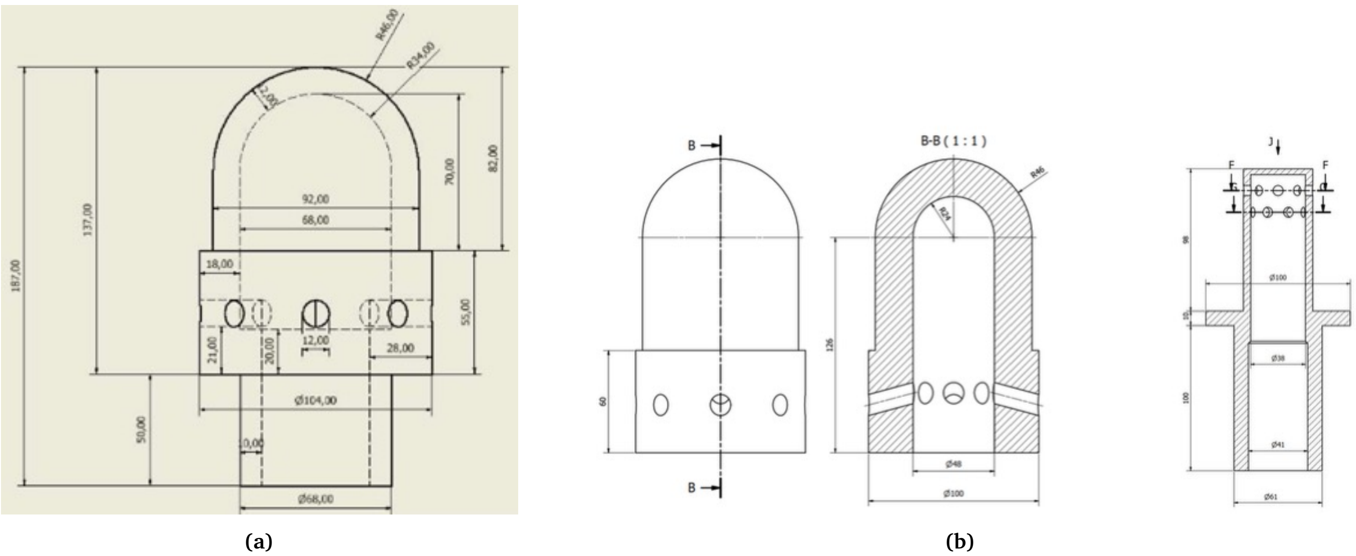

Figure 1. The air-caps used in this study: (a) conventional bell-type air-cap and (b) innovative bell-type air-cap. All geometric dimensions are presented in millimeters (mm) to ensure reproducibility. The innovative design is characterized by modified geometry to enhance air distribution uniformity and reduce localized jet penetration.

expansion, and the apparent onset of fluidization [2].

The novelty of this study lies in the direct experimental comparison of conventional and innovative bell-type air-cap geometries using the same cold-flow apparatus and operating conditions. The comparison was conducted with Geldart B silica sand and Geldart D low-rank coal at different initial bed heights. In addition to quantifying the pressure-loss differences between the two designs, the study examines material-dependent bed behavior and compares the experimentally identified apparent minimum fluidization velocity with predictions from established correlations.

This research aims to evaluate the influence of bell-type air-cap geometry on pressure loss and bed behavior under cold-flow conditions. Specifically, it quantifies the pressure-drop reduction produced by the innovative design, determines the apparent minimum fluidization velocity (U_{mf}) of silica sand, characterizes the partial particle movement observed in the low-rank-coal bed, and assesses the applicability of the Wen–Yu, Basu, and Ergun-based correlations. The findings provide experimental hydrodynamic evidence for the further development of primary-air distributors in CFB systems.

2. Material and Method

2.1. Material

The materials used in this study were silica sand and low-rank coal. The composition of silica sand was SiO_2 99.2%-wt, with an average size of 706 μm, and it was obtained from a commercial supplier. The low-rank coal was obtained from coal stockpiles in Serang City-Banten. The coal size was reduced according to the SNI ASTM C136-2012 method.

2.2. Preparation of Material

The bed materials, silica sand and low-rank coal, were prepared and stored separately in labeled containers to prevent material mixing and moisture contamination. The coal was classified into the required particle-size fractions using a sieve shaker, and each fraction was stored in a separate container with information on material type and particle size. Furthermore, the silica sand and coal bed materials were weighed alternately according to the variation in the bed height. This preparation ensures reproducibility of particle size distribution and uniform initial bed conditions, which are critical for determining minimum fluidization velocity (U_{mf}) and pressure drop (ΔP).

2.3. Experimental Setup

The experiment was conducted in a box-shaped fluidization column (32 cm $\times$ 32 cm $\times$ 200 cm) equipped with a forced draft (FD) fan, an air-cap distributor, a U-tube manometer, a Variable Frequency Drive (VFD) inverter operating at 10–50 Hz, and an anemometer installed inside the air-supply pipe. The bed material was loaded at initial heights of 30 cm and 40 cm. Airflow was supplied by the FD fan and regulated by adjusting the fan frequency using the VFD inverter. For each frequency setting, the air velocity inside the supply pipe was recorded using the anemometer, and the corresponding volumetric airflow rate was calculated by multiplying the measured pipe velocity by the internal cross-sectional area of the pipe. The superficial gas velocity (U) in the fluidization chamber was subsequently determined by dividing the calculated volumetric airflow rate by the cross-sectional area of the fluidization column. Over the FD-fan frequency range of 10–50 Hz, the resulting superficial gas velocity in the fluidization chamber ranged from 7.94 to 38.25

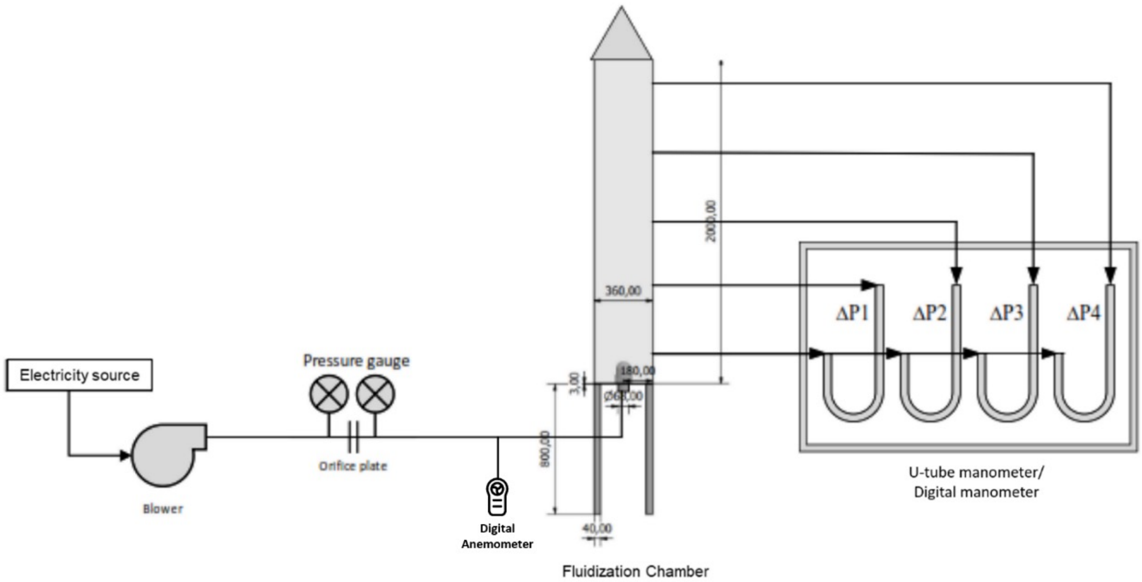

Figure 2. Experimental equipment setup used in this study; all dimensional specifications are expressed in millimeters (mm).

cm/s. The onset of fluidization was identified based on the observed bed expansion and changes in pressure drop represented by the ($\Delta P - U$) curve.

Pressure drops across the distributor and the gas–solid bed was measured using both U-tube and digital manometers. The U-tube manometer determines the static pressure difference between two gas-phase pressure taps through the hydrostatic balance of the manometric liquid. Because the pressure taps communicate with the interstitial gas phase, the measured value represents the gas-phase pressure loss generated by the distributor and the gas–solid bed rather than the particle pressure itself. The digital manometer provided direct differential-pressure readings and was used to support verification of the U-tube measurements. Time-averaged readings were recorded under each airflow condition to represent the bulk gas–solid hydrodynamic response and to reduce the influence of short-term pressure fluctuations. Pressure drop and bed height were documented systematically to maintain data consistency and experimental repeatability. The experiments were conducted sequentially for the air–silica sand system (Geldart group B) and the air–coal system (Geldart group D), to evaluate their behavior in the fixed-bed, transition, and fluidization regimes.

2.4. Minimum Fluidization Velocity (U_{mf})

The minimum fluidization velocity (U_{mf}) was estimated using several empirical correlations to provide a comparative theoretical framework for evaluating experimental results under different particle systems. The minimum fluidization velocity was first estimated using the Wen–Yu correlation, which relates the Reynolds number at minimum fluidization ($N_{Re_{mf}}$) to the Archimedes number (N_{Ar}) or Galileo number (N_{Ga}). This correlation is widely used because it provides a generalized estimation of U_{mf} based on particle diameter, gas density, gas viscosity, particle density, and gravitational acceleration [4].

$$\frac{d_p U_{mf} \rho_g}{\mu_g} = \left(C_1^2 + C_2 \frac{d_p^3 \rho_g (\rho_p - \rho_g) g}{\mu_g^2} \right)^{\frac{1}{2}} - C_1 \tag{1}$$

The value of C_1 and C_2 are 33.7 and 0.0408 respectively. This formulation assumes spherical particles and homogeneous distribution within the bed.

In addition, Basu [5] proposed an empirical correlation from the Wen-Yu correlation for estimating U_{mf}, with constants C_1 and C_2 of 30.28 and 0.046, which is widely applied in industrial fluidized bed systems due to its robustness in handling a wide range of particle sizes and densities. These constants originate from regression analysis of extensive experimental datasets and represent the balance between viscous and inertial forces during fluidization. The Ergun equation is also used to estimate the pressure drop at the onset of fluidization [6]. This equation provides a fundamental relationship between pressure drop and superficial gas velocity in packed and fluidized beds, representing both viscous and kinetic energy losses.

$$\frac{\Delta P}{L} = 150 \frac{(1-\varepsilon)^2}{\varepsilon^3} \frac{\mu_g U_{mf}}{(\phi d_p)^2} + 1.75 \frac{(1-\varepsilon)^2}{\varepsilon^3} \frac{\rho_g U_{mf}^2}{\phi d_p} \tag{2}$$

The first term represents the viscous contribution to pressure loss and is proportional to the superficial gas velocity. This contribution is particularly important at relatively low gas velocities and in densely packed particle beds, where fluid resistance is predominantly governed by gas viscosity and interstitial flow through the void spaces. The second term represents the inertial contribution and is proportional to the square of the superficial gas velocity. Its influence becomes increasingly significant as the gas velocity increases. The onset of fluidization is identified when the pressure drop approaches a nearly constant value or plateau, indicating that the gas drag force has become sufficient to support the effective weight of the bed. Thus, the Ergun equation provides the theoretical basis for interpreting the pre-fluidization pressure-drop behavior and estimating the minimum fluidization condition.

2.5. Uncertainty Analysis

Uncertainty analysis was conducted using a Type A approach based on duplicate pressure-drop measurements. Experimental uncertainty represents the random variation observed among repeated measurements and is distinct from systematic error associated with persistent instrument bias, calibration error, or deficiencies in the measurement procedure. Repeated observations provide a statistical basis for estimating experimental repeatability and the uncertainty of the reported mean [7]. This treatment is also consistent with the general uncertainty framework of Kline and McClintock [8], which requires the uncertainty associated with each measured variable to be identified before the reliability of an experimental result is assessed.

For each operating point j, two pressure-drop measurements, $\Delta P_{1,j}$ and $\Delta P_{2,j}$, were obtained under identical conditions of material, initial bed height, blower frequency, and pressure-tapping position. Therefore, the number of repeated measurements at each operating point was $n = 2$. A total of $N = 20$ paired operating points was evaluated for each material–bed-height group.

The mean pressure drop for the jth operating point was calculated as:

$$\overline{\Delta P}_j = \frac{\Delta P_{1,j} + \Delta P_{2,j}}{2} \tag{3}$$

The absolute difference between the duplicate measurements was determined from:

$$d_{\Delta P,j} = |\Delta P_{1,j} - \Delta P_{2,j}| \tag{4}$$

The sample standard deviation of the duplicate pressure-drop measurements was calculated as:

$$s_{\Delta P,j} = \left[\frac{\sum_{i=1}^{n} \left(\Delta P_{i,j} - \overline{\Delta P}_j \right)^2}{n-1} \right]^{\frac{1}{2}} \tag{5}$$

The Type A standard uncertainty of the pairwise mean was calculated according to Young (1962):

$$u_A \left(\overline{\Delta P}_j \right) = \frac{s_{\Delta P,j}}{\sqrt{n}} \tag{6}$$

The relative Type A standard uncertainty was expressed as:

$$u_{r,A} \left(\overline{\Delta P}_j \right) = \frac{u_A \left(\overline{\Delta P}_j \right)}{\overline{\Delta P}_j} \times 100\% \tag{7}$$

The relative percent difference was calculated as:

$$RPD_j = \frac{|\Delta P_{1,j} - \Delta P_{2,j}|}{\overline{\Delta P}_j} \times 100\% \tag{8}$$

For a duplicate pair, Equations (6)–(8) give the following relationship:

$$RPD_j = 2u_{r,A} \left(\overline{\Delta P}_j \right) \tag{9}$$

For each material–bed-height group, the arithmetic mean of a pairwise parameter Y_j was calculated from the $N = 20$ operating points as:

$$\overline{Y} = \frac{1}{N} \sum_{j=1}^{N} Y_j \tag{10}$$

where Y_j represents $\overline{\Delta P}_j$, $d_{\Delta P,j}$, $s_{\Delta P,j}$, or $u_A \left(\overline{\Delta P}_j \right)$. Consequently, the mean pairwise Type A standard uncertainty reported in Table 3 is the arithmetic mean of the 20 individual pairwise uncertainty values and should not be interpreted as the standard uncertainty of a single grand mean.

The median and maximum relative Type A standard uncertainties were determined as:

$$\widetilde{u}_{r,A} = \text{median} \left[u_{r,A,1}, u_{r,A,2}, \ldots, u_{r,A,N} \right] \tag{11}$$

$$u_{r,A,\max} = \max \left[u_{r,A,1}, u_{r,A,2}, \ldots, u_{r,A,N} \right] \tag{12}$$

Similarly, the median and maximum RPD values were calculated as:

$$\widetilde{RPD} = \text{median} \left[RPD_1, RPD_2, \ldots, RPD_N \right] \tag{13}$$

$$RPD_{\max} = \max \left[RPD_1, RPD_2, \ldots, RPD_N \right] \tag{14}$$

Because only two repeated measurements were obtained at each operating point, each duplicate pair provides one statistical degree of freedom. The resulting Type A standard uncertainties should therefore be interpreted as repeatability-based estimates of random experimental variation with limited statistical confidence [7].

3. Results and Discussion

3.1. Material Bed Characterization

The physical properties of silica sand and low-rank coal, as summarized in Table 1, show significant differences that affect fluidization behavior, particularly minimum fluidization velocity (U_{mf}) and pressure drop (ΔP). Silica sand exhibits a higher bulk density (1420 kg/m^3), while coal shows a lower bulk density (640 kg/m^3), depending on its moisture content [9,10]. These differences strongly affect drag force balance and fluidization onset, where higher density particles generally require higher superficial gas velocity (U) to achieve fluidization.

The two materials also differed substantially in particle-size distribution. Silica sand had an average particle size of 706 μm and a comparatively narrower distribu-

Table 1. Characteristics of the bed material used in this study.

Material bed	Bulk Density (kg/m^3)	Particle Size Distribution (PSD) (mesh)	(%-wt)
Silica Sand	1420	20	8.62
		-20 + 35	29.06
		-35 +30	10.94
		-30	51.38
Low-rank Coal	640	< 4	0.06
		-4–5	0.10
		5–7	0.50
		7–10	14.01
		10–20	81.57
		> 20	3.75

tion, which favors a more consistent hydrodynamic response. Low-rank coal had a larger average particle size of approximately 1470 μm and a broader distribution. These characteristics can produce unequal particle entrainment, size segregation, and localized bed movement because particles of different sizes experience different drag forces [11]. Consequently, the coal bed may require a higher superficial gas velocity than the silica-sand bed to approach fluidization.

Particle-size distribution and packed-bed structure influence the local void fraction (ε), gas-flow resistance, and pressure-drop–velocity ($\Delta P - U$) response. In the fixed-bed regime, these effects are represented by the viscous and inertial contributions of the Ergun equation [12]. Therefore, differences in material properties must be considered when comparing the measured pressure-drop responses of the two air-cap designs.

Silica sand is commonly used in fluidized-bed studies because its comparatively regular particles and relatively narrow particle-size distribution generally produce a reproducible transition from fixed-bed to fluidized-bed conditions [6,12,13]. In the present study, these characteristics were consistent with the identifiable pressure-drop transition and observable bed expansion obtained for silica sand. The results should not, however, be interpreted as direct evidence of spatially uniform airflow because local gas-velocity profiles were not measured.

Low-rank coal presents additional cold-flow challenges associated with its broad particle-size distribution, irregular particle characteristics, and moisture-related interparticle forces [14]. Smaller particles may begin to move before larger particles, resulting in localized movement, channeling, or segregation rather than simultaneous full bed fluidization [15]. Under the tested superficial-gas-velocity range, only partial particle movement was observed, and no stable pressure-drop plateau was obtained. Therefore, an experimental U_{mf} for low-rank coal could not be determined reliably.

Variations in particle size, particle-size distribution, and packed-bed density can alter gas–solid hydrodynamics in CFB systems [16]. The narrower particle-size distribution of silica sand supported a more consistent bed response, whereas the broader distribution and interparticle forces of low-rank coal hindered collective bed movement. Accordingly, the performance of an air-cap should be evaluated for the intended bed material rather than inferred solely from tests conducted with an ideal or single particle system.

The bed-material characterization results demonstrate that bed-material properties strongly influence the pressure-drop response and the transition toward fluidization. Silica sand exhibited a clearer and more reproducible transition because of its smaller average particle size and narrower particle-size distribution. In contrast, low-rank coal was more difficult to fluidize because of its larger average particle size, broader distribution, and moisture-related interparticle forces. These differences provide the basis for interpreting the material-dependent $\Delta P - U$ responses presented in the following sections.

3.2. Fluidization Characteristics Curve of Silica Sand

The pressure-drop response of the silica-sand bed was evaluated using conventional and innovative bell-type air-caps at initial bed heights of 30 and 40 cm, as shown in Figure 3. In the fixed-bed region, the measured pressure drop (ΔP) increased with superficial gas velocity (U) because of the increasing resistance to gas flow through the packed particles. An apparent minimum fluidization velocity (U_{mf}) of approximately 30.67 cm/s was identified from the change in the slope of the $\Delta P - U$ response, supported by the observed bed expansion. Above this transition, the pressure drop tended to level off or decrease slightly, indicating that the gas drag had become sufficient to support and mobilize the silica-sand bed. This trend is consistent with the transition from packed-bed flow described by the Ergun equation to the fluidized-bed regime.

At the apparent minimum fluidization velocity of 30.67 cm/s, the innovative bell-type air-cap produced a lower measured pressure loss than the conventional de-

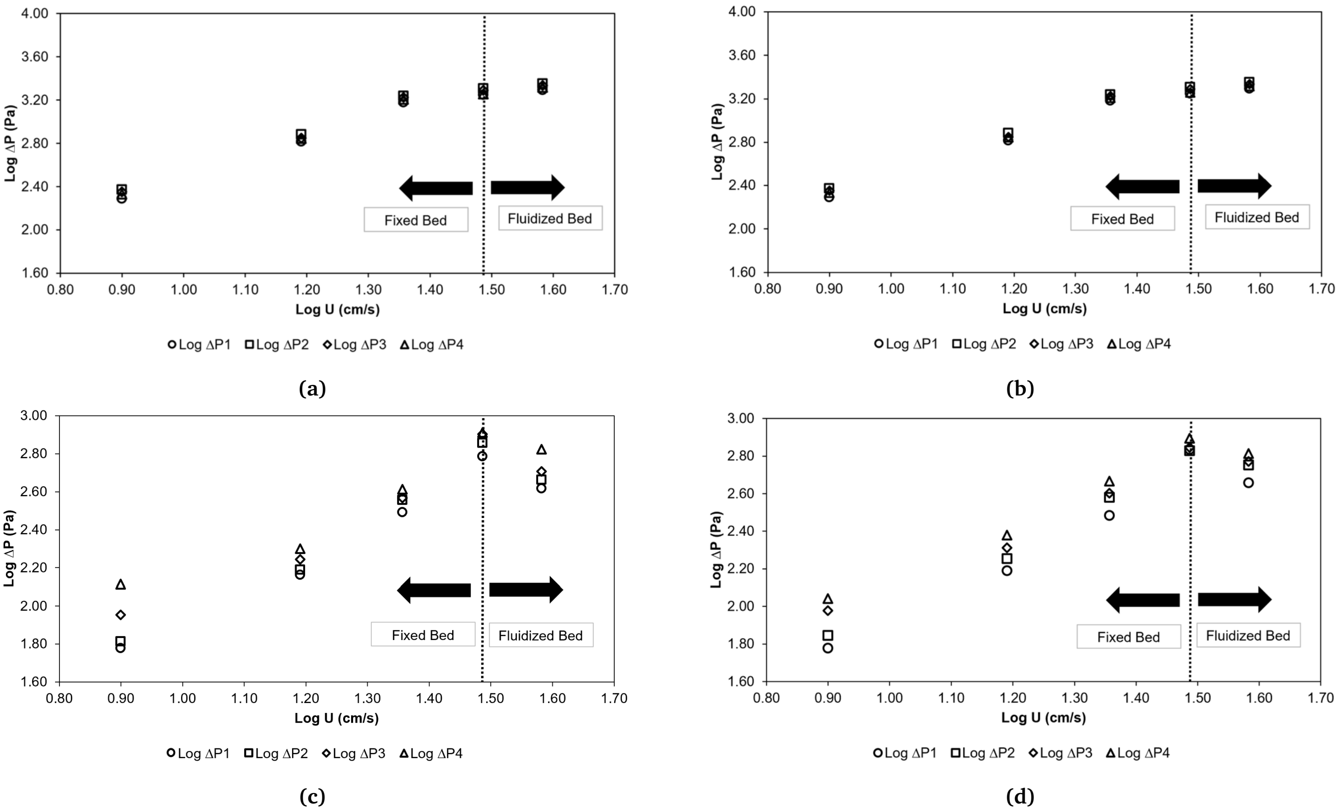

Figure 3. Fluidization characteristics curve of silica sand using conventional air-cap bell type at initial bed heights of (a) 30 cm and (b) 40 cm and the innovative air-cap bell type at initial bed heights of (c) 30 cm and (d) 40 cm. The symbols represent measurements at the four pressure-tapping locations (ΔP_1–ΔP_4), and the vertical dotted line indicates the apparent minimum fluidization velocity of approximately 30.67 cm/s.

sign. The reduction ranged from 11.9% to 16.6% across the four pressure-tapping locations (ΔP_1–ΔP_4). This result demonstrates that the modified air-cap geometry reduced the measured resistance to gas flow under comparable operating conditions. For the initial bed height of 40 cm, the silica-sand bed expanded to approximately 42.5 cm, supporting the identification of the transition to fluidization. However, the lower pressure drop alone does not directly demonstrate improved spatial airflow uniformity because local gas-velocity distributions were not measured.

The observed pressure-drop trend is consistent with previous studies showing that air-cap geometry influences distributor resistance and gas delivery into fluidized beds [1–3]. As shown in Figures 3(c) and 3(d), the innovative air-cap generally produced lower ΔP values than the conventional configuration. The responses recorded at the four pressure-tapping locations may indicate a more even overall hydrodynamic response; nevertheless, this interpretation remains indirect because neither local gas velocity nor jet penetration was measured in the present experiments.

The observed bed expansion provides additional evidence that the silica-sand particles transitioned from a packed condition to a mobile fluidized state [13]. For the 40 cm initial bed, the increase in bed height to approximately 42.5 cm occurred near the apparent U_{mf}. When considered together with the change in the $\Delta P - U$ response, this expansion confirms the onset of fluidization. The simultaneous occurrence of bed expansion and lower measured pressure loss indicates that the innovative air-cap achieved particle mobilization with less pressure resistance than the conventional design, although the degree of gas–solid contact uniformity was not quantified directly.

The measured pressure-loss reduction of 11.9–16.6% indicates that the innovative air-cap required a lower pressure difference to reach the apparent fluidization condition of the silica-sand bed. In a practical air-supply system, a lower pressure requirement at a comparable volumetric flow rate may provide an opportunity to reduce blower duty. However, actual energy savings cannot be quantified from the present results because blower efficiency and electrical power consumption were not measured. Therefore, the demonstrated advantage of the innovative design is limited to its lower measured pressure loss under the tested cold-flow conditions.

3.3. Fluidization Characteristics Curve of Coal

The pressure-drop response of the low-rank-coal bed differed substantially from that of silica sand, as shown in Figure 4. For both air-cap designs, the measured pressure

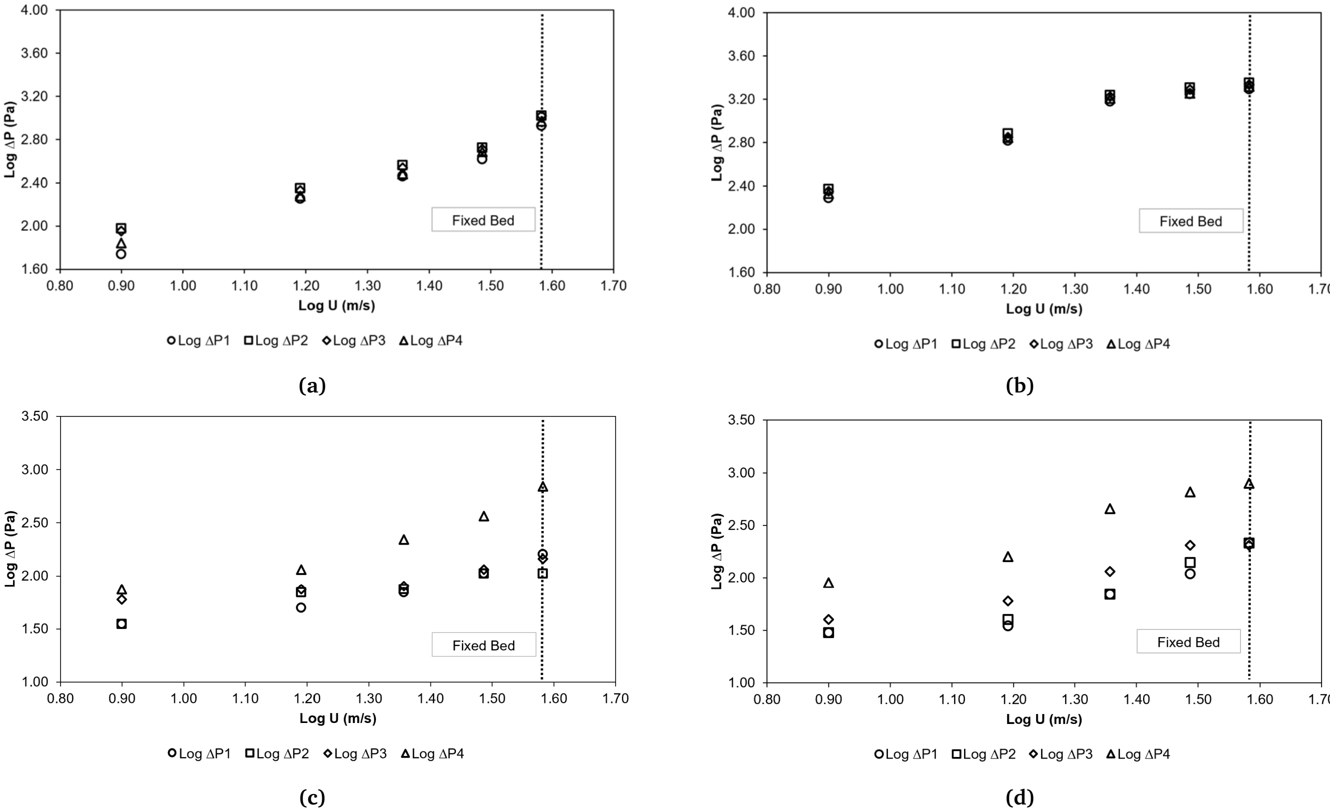

Figure 4. Fluidization characteristics curve of coal using conventional air-cap bell type at initial bed heights of (a) 30 cm and (b) 40 cm and innovative air-cap bell type at initial bed heights of (c) 30 cm and (d) 40 cm. The symbols represent measurements at the four pressure-tapping locations (ΔP_1–ΔP_4). The vertical dotted line indicates the maximum superficial gas velocity tested rather than the onset of fluidization.

drop (ΔP) increased continuously with superficial gas velocity (U) over the tested range of 7.94–38.25 cm/s. No stable pressure-drop plateau or sustained full-bed expansion was observed. Therefore, the coal bed remained predominantly in the fixed-bed regime, although localized particle movement was visually observed at the higher gas velocities. Because full-bed fluidization was not achieved, an experimental minimum fluidization velocity (U_{mf}) could not be determined for low-rank coal.

The absence of full fluidization within the available velocity range indicates that the U_{mf} of the low-rank-coal bed, if attainable under the present conditions, would exceed the maximum tested velocity of 38.25 cm/s. This value should therefore be interpreted only as a lower experimental limit and not as the coal U_{mf}. Figures 4(c) and 4(d) show that the innovative air-cap generally produced lower measured pressure drops than the conventional design. However, the results do not directly demonstrate improved airflow uniformity because local gas-velocity distributions were not measured. Furthermore, the modified air-cap did not produce a stable pressure-drop plateau or full-bed fluidization.

The difficulty in fluidizing low-rank coal may be associated with its larger average particle size, broad particle-size distribution, irregular particle characteristics, and moisture-related interparticle forces [17, 18]. These properties can cause particles of different sizes to respond differently to the applied gas drag, resulting in localized movement, channeling, or temporary clustering rather than collective bed suspension. Because the experiments were performed under cold-flow conditions, the observed behavior should not be attributed to thermally induced ash agglomeration. The continuously increasing ΔP response in Figure 4 confirms that the available airflow was insufficient to establish a stable fluidized-bed regime.

The results indicate that a higher superficial gas velocity would be required to overcome the resistance and interparticle forces within the coal bed. However, the additional velocity and pressure requirements necessary to achieve full fluidization cannot be quantified from the present data because the experimental system did not reach the coal U_{mf}. Although the innovative air-cap produced lower measured pressure losses at several pressure-tapping locations, this observation provides only indirect evidence of a different hydrodynamic response. It does not confirm the elimination of localized high-pressure regions or flow maldistribution without direct local-velocity measurements.

Coal agglomeration further contributes to bed instability and makes homogeneous fluidization difficult to achieve [20]. Although the innovative air-cap improved air distribution, the dominant limitation remained the in-

Table 2. Comparison of experimental and theoretical U_{mf} values.

Material Bed	Height (cm)	U_{mf} (cm/s)				Absolute Relative Error (%)		
		This work	Wen–Yu	Basu	Ergun	Wen–Yu	Basu	Ergun
Silica Sand	30	30.67	34.56	40.91	6.12	12.7%	33.4%	80.1%
	40	30.67	34.56	40.91	6.12	12.7%	33.4%	80.1%

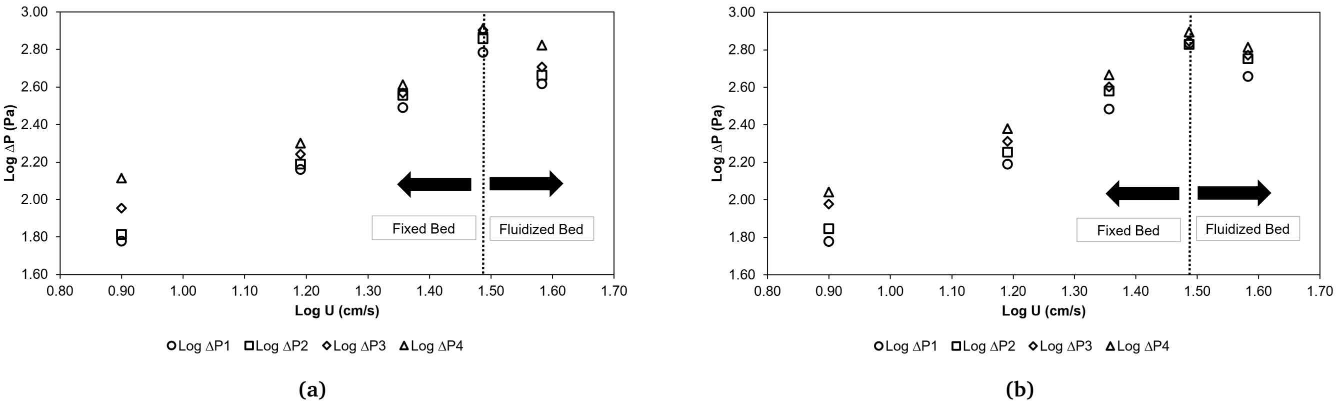

Figure 5. Fluidization characteristic curve of silica sand at initial bed height (a) 30 cm (b) 40 cm.

trinsic behavior of coal particles, including cohesion, broad PSD, and agglomeration. Therefore, air-cap modification alone is not sufficient to fully overcome the fluidization limitations of Geldart D-type coal particles.

3.4. Minimum Fluidization Velocity (U_{mf})

Figure 5 presents the logarithmic pressure-drop–velocity responses of the silica-sand bed at initial bed heights of 30 and 40 cm. At low superficial gas velocities, the pressure drop (ΔP) increased with U, indicating that the bed remained in the fixed-bed regime. The apparent minimum fluidization velocity (U_{mf}) was assigned to the tested velocity at which the increasing pressure-drop trend changed, and visible bed expansion began. Based on these combined pressure-drop and visual observations, the apparent U_{mf} was approximately 30.67 cm/s for both initial bed heights. At the subsequent higher velocity, the measured pressure drop decreased slightly, which is consistent with particle rearrangement and increasing bed voidage after the onset of fluidization.

Table 2 compares the experimentally identified apparent U_{mf} with values predicted using the Wen–Yu correlation [4], the Wen–Yu-type correlation with constants reported by Basu [5], and the Ergun-based calculation. The theoretical calculations were performed using consistent SI units, and the resulting velocities were converted to cm/s for comparison with the experimental data. The Wen–Yu and Basu correlations predicted U_{mf} values of 34.56 and 40.91 cm/s, respectively, and therefore overpredicted the experimental value of 30.67 cm/s. In contrast, the Ergun-based calculation yielded 6.12 cm/s and substantially underpredicted the experimental result. The corresponding absolute relative errors were 12.7%, 33.4%, and 80.1%, respectively.

The silica-sand bed exhibited a clearly identifiable transition because of its comparatively smaller average particle size, narrower particle-size distribution, and limited interparticle cohesion. In contrast, the low-rank-coal bed exhibited only localized particle movement and did not develop a stable pressure-drop plateau within the tested velocity range. Consequently, an experimental U_{mf} could be identified for silica sand but could not be determined reliably for low-rank coal. The coal U_{mf}, if attainable under the present bed conditions, would exceed the maximum tested superficial gas velocity of 38.25 cm/s.

Among the evaluated methods, the Wen–Yu correlation provided the closest prediction of the experimental apparent U_{mf}. The larger deviation obtained using the Basu correlation resulted from its higher predicted velocity, whereas the Ergun-based method substantially underestimated U_{mf}. These deviations may reflect differences between the experimental bed and the idealized assumptions embedded in the correlations, including spherical and uniformly sized particles, homogeneous packing, specified bed voidage, and negligible wall effects. The rectangular column geometry measured particle-size distribution, uncertainty in particle sphericity and bed voidage, and the discrete velocity increments used to identify the transition may also have contributed to the observed differences.

The same apparent U_{mf} of 30.67 cm/s was obtained for the 30 and 40 cm silica-sand beds. This result indicates that no detectable effect of initial bed height on the apparent U_{mf} was observed within the tested conditions and the resolution of the applied velocity increments.

Table 3. Repeatability-based Type A uncertainty of pressure-drop measurements for silica sand and low-rank coal.

Material	Initial bed, H_0 (cm)	Paired points, N	Mean pressure drop, ΔP (Pa)	Mean absolute difference, $\overline{\lvert\Delta P\rvert}$ (Pa)	Mean pairwise sample SD, $s_{\Delta P}$ (Pa)	Mean pairwise Type A uncertainty standard, $u_A(\overline{\Delta P})$ (Pa)	Median relative u_A (%)	Maximum relative u_A (%)	Median RPD (%)	Maximum RPD (%)
Silica Sand	30	20	373.25	15.50	10.96	7.75	2.57	16.67	5.14	33.33
	40	20	388.50	17.00	12.02	8.50	1.40	14.75	2.79	29.51
Low-Rank Coal	30	20	137.75	15.50	10.96	7.75	6.67	16.67	13.33	33.33
	40	20	186.75	15.50	10.96	7.75	6.61	33.33	13.23	66.67

It should not be interpreted as evidence that bed height has no influence under all operating conditions, because increasing the bed inventory still affects the total pressure-drop magnitude and expanded-bed height.

3.5. Uncertainty Analysis

The repeatability-based uncertainty assessment provides a quantitative basis for evaluating the internal consistency of the pressure-drop measurements. A Type A approach was applied to duplicate observations obtained under the same bed-material, initial-bed-height, blower-frequency, and pressure-tapping conditions [21]. The assessment included the pairwise mean pressure drop, absolute difference between duplicate readings, sample standard deviation, Type A standard uncertainty of the pairwise mean, relative Type A standard uncertainty, and relative percent difference (RPD). These statistics quantify random variation under repeatability conditions but do not include systematic contributions associated with instrument calibration, measurement bias, or experimental procedure. Because repeated superficial-gas-velocity measurements were not available, the present uncertainty analysis was limited to the pressure-drop data. The use of duplicate-measurement statistics is consistent with established approaches for estimating measurement repeatability from the absolute and relative differences between paired observations [22].

For silica sand, the duplicate pressure-drop measurements showed comparatively good repeatability. The mean pairwise pressure drop increased from 373.25 Pa at an initial bed height of 30 cm to 388.50 Pa at 40 cm. The mean pairwise Type A standard uncertainties, calculated using Equations (6) and (10), were 7.75 and 8.50 Pa for the 30 and 40 cm beds, respectively. Because absolute uncertainty depends on the magnitude of the measured pressure drop, the relative statistics provide a more appropriate basis for comparison. The median relative Type A standard uncertainties were 2.57% at 30 cm and 1.40% at 40 cm, while the corresponding median RPD values were 5.14% and 2.79%. These low median values indicate limited random variation for most duplicate observations. However, the maximum relative Type A standard uncertainties reached 16.67% and 14.75%, with maximum RPD values of 33.33% and 29.51%, respectively. These isolated higher values indicate that several operating points experienced greater short-term variability, potentially because of particle rearrangement, intermittent bubbling near or above the onset of fluidization, local voidage changes, and transient gas–solid momentum exchange [12, 13].

Low-rank coal exhibited greater relative variation than silica sand. Although the mean absolute differences at initial bed heights of 30 and 40 cm were both 15.50 Pa, the corresponding mean pressure drops were only 137.75 and 186.75 Pa, respectively. Consequently, similar absolute differences resulted in larger relative Type A uncertainties. The mean pairwise Type A standard uncertainty was 7.75 Pa for both bed heights. The median relative Type A standard uncertainties, calculated using Equations (7) and (11), were 6.67% and 6.61% at 30 and 40 cm, respectively, while the corresponding median RPD values were 13.33% and 13.23%. The maximum relative Type A uncertainty increased from 16.67% at 30 cm to 33.33% at 40 cm, corresponding to maximum RPD values of 33.33% and 66.67%, respectively. These results indicate that several individual measurements exhibited substantially greater random variation than the group median. This behavior may be associated with the heterogeneous characteristics of low-rank coal, including its broad particle-size distribution, irregular particle shape, moisture-related cohesion, interparticle bonding, and tendency to agglomerate.

The uncertainty statistics provide a quantitative basis for assessing the reliability of the measured pressure-drop trends and the comparison between the two air-cap designs. The relatively low median uncertainties obtained for silica sand indicate greater internal consistency than those obtained for low-rank coal. The measured pressure-loss reduction produced by the innovative air-cap should therefore be interpreted together with the uncertainty at the corresponding operating point. For silica sand, the reported reduction of 11.9–16.6% was substantially greater than the group median relative Type A uncertainty of 1.40–2.57%, although isolated maximum uncertainty values were of a comparable magnitude. The low-rank-coal results require greater caution because their relative uncertainties were higher and full-bed fluidization was not achieved. These Type A values represent repeatability-based random variation only and should not be interpreted as complete measurement uncertainties or as direct evidence of model accuracy.

Because only two measurements were obtained at each operating point, each duplicate pair provided one statistical degree of freedom. Consequently, the Type A standard uncertainties reported in Table 3 have limited statistical confidence and primarily describe short-term measurement repeatability. Additional independent repetitions and repeated superficial-gas-velocity measurements are recommended to provide a more comprehensive assessment of experimental uncertainty.

4. Conclusions

In this study, the silica-sand bed reached an apparent minimum fluidization velocity (U_{mf}) of approximately 30.67 cm/s at initial bed heights of 30 and 40 cm. The identical values indicate that no detectable influence of bed height on the apparent U_{mf} was observed within the tested range and the resolution of the applied velocity increments. In contrast, low-rank coal exhibited only localized particle movement at higher superficial gas velocities, without a stable pressure-drop plateau or sustained full-bed expansion. Consequently, an experimental U_{mf} could not be determined for the coal bed within the available velocity range of 7.94–38.25 cm/s. This behavior was associated with the larger average particle size, broader particle-size distribution, irregular particle characteristics, and moisture-related interparticle forces of the low-rank coal. At the apparent U_{mf} of silica sand, the innovative bell-type air-cap reduced the measured pressure loss by 11.9–16.6% across the four pressure-tapping locations (ΔP_1–ΔP_4) relative to the conventional design. This result demonstrates lower measured flow resistance and suggests the potential to reduce the pressure requirement of the air-supply system. However, airflow uniformity, localized jet penetration, FD-fan power, and energy consumption were not measured directly; therefore, improvements in these parameters cannot be quantified from the present results. The Wen–Yu correlation provided the closest prediction of the experimental apparent U_{mf}, with an absolute relative error of 12.7%. The Basu correlation overpredicted U_{mf}, producing an error of 33.4%, whereas the Ergun-based calculation substantially underpredicted it, with an error of 80.1%. Thus, the Wen–Yu correlation showed the best agreement among the three evaluated methods, although the remaining deviation indicates that particle-size distribution, bed packing, particle sphericity, voidage, wall effects, and other experimental conditions influence prediction accuracy.

The Type A analysis showed better repeatability for the silica-sand pressure-drop measurements than for the low-rank-coal measurements; however, the estimates were based on only two repetitions at each operating point and therefore had limited statistical confidence. Future studies should conduct at least three independent repetitions of both pressure-drop and superficial-gas-velocity measurements at every operating condition. Direct measurements of local gas-velocity distribution, nozzle discharge behavior, volumetric flow rate, FD-fan efficiency, and electrical power consumption are also recommended to verify airflow uniformity and quantify potential energy savings. Extending the available gas-velocity range and controlling coal moisture content and particle-size distribution would further support reliable determination of the coal U_{mf} and evaluation of the innovative air-cap under more representative operating conditions.

Nomenclature

Terms	Notes	Unit
ΔP	Pressure drop across the bed or air-cap distributor	Pa
U	Superficial gas velocity	m/s
U_{mf}	Minimum fluidization velocity	m/s
H_0	Initial bed height	m
H_f	Fluidized-bed height or expanded-bed height	m
d_p	Particle or solid diameter	m
ρ_g	Gas density	kg/m^3
ρ_p	Particle or solid density	kg/m^3
ρ_{bulk}	Bulk density of bed material	kg/m^3

Terms	Notes	Unit
μ_g	Dynamic viscosity of gas	Pa·s
ε	Void fraction of the bed	–
ϕ	Sphericity of bed particles	–
g	Gravitational acceleration	m/s^2
C_1	Empirical constant in the minimum fluidization velocity correlation	–
C_2	Empirical constant in the minimum fluidization velocity correlation	–
$\Delta P_{i,j}$	The ith pressure-drop measurement at the jth operating point	Pa
$\Delta P_{1,j}$	First pressure-drop measurement at the jth operating point	Pa
$\Delta P_{2,j}$	Second pressure-drop measurement at the jth operating point	Pa
$\overline{\Delta P}_j$	Mean of the duplicate pressure-drop measurements at the jth operating point	Pa
$d_{\Delta P,j}$	Absolute difference between duplicate pressure-drop measurements at the jth operating point	Pa
$s_{\Delta P,j}$	Sample standard deviation of duplicate pressure-drop measurements at the jth operating point	Pa
$u_A\left(\overline{\Delta P}_j\right)$	Type A standard uncertainty of the pairwise mean pressure drop at the jth operating point	Pa
$u_{r,A}\left(\overline{\Delta P}_j\right)$	Relative Type A standard uncertainty of the pairwise mean pressure drop at the jth operating point	%
RPD_j	Relative percent difference between duplicate pressure-drop measurements at the jth operating point	%
Y_j	Pairwise pressure-drop statistics evaluated at the jth operating point	Pa
$\overline{Y}$	Arithmetic mean of a pairwise pressure-drop statistic over N operating points	Pa
$\widetilde{u}_{r,A}$	Median relative Type A standard uncertainty	%
$u_{r,A,\max}$	Maximum relative Type A standard uncertainty	%
$\widetilde{RPD}$	Median relative percent difference	%
$RPD_{\max}$	Maximum relative percent difference	%
n	Number of repeated measurements at each operating point	–
N	Number of paired operating points in each material–bed-height group	–
i	Index of repeated measurements within an operating point	–
j	Index of operating points	–

Acknowledgments

The author would like to thank the Institute of Research and Community Service (LPPM) of University of Sultan Ageng Tirtayasa for the research grant based on the 2024 PDP Research Grant.

References

[1] X. Liu, G. Zhu, T. Asim, Y. Zhang, and R. Mishra, "The innovative design of air caps for improving the thermal efficiency of CFB boilers," *Energy*, vol. 221, p. 119844, 2021.

[2] Z. Huang, L. Deng, and D. Che, "Experimental and CFD simulation studies on bell-type air nozzles of CFB boilers," *Applied Sciences*, vol. 9, no. 18, p. 3805, 2019.

[3] P. Mirek, "Air distributor pressure drop analysis in a circulating fluidized-bed boiler for non-reference operating conditions," *Chemical Engineering & Technology*, vol. 43, no. 11, pp. 2233–2246, 2020.

[4] C. Y. Wen and Y. H. Yu, "A generalized method for predicting the minimum fluidization velocity," *AIChE Journal*, vol. 12, no. 3, pp. 610–612, 1966.

[5] P. Basu, *Circulating Fluidized Bed Boilers: Design, Operation and Maintenance*. Cham: Springer International Publishing, 2015.

[6] S. Ergun, "Fluid flow through packed columns," *Chemical Engineering Progress*, vol. 48, no. 2, pp. 89–94, 1952.

[7] H. D. Young, *Statistical Treatment of Experimental Data*. New York: McGraw-Hill Book Company, Inc., 1962.

[8] S. J. Kline and F. A. McClintock, "Describing uncertainties in single-sample experiments," *Mechanical Engineering*, vol. 75, no. 1, pp. 3–8, 1953.

[9] A. C. Sivri, "Fluidization behavior of binary mixtures of coal in a top-fed bubbling fluidized bed gasifier," in *Recent Advances for Coal Energy in the 21st Century* (Y. Yun, ed.), IntechOpen, 2023.

[10] S. Rianda, D. Yaskuri, and M. A. A. Efendi, "Low-rank coal gasification using a bubbling fluidized bed reactor at low operating temperature," *Indonesian Mining Journal*, vol. 22, no. 2, pp. 99–105, 2019.

[11] X. Liu, H. Yang, and J. Lyu, "Optimization of fluidization state of a circulating fluidized bed boiler for economical operation," *Energies*, vol. 13, no. 2, p. 376, 2020.

[12] S. S. Ali, S. K. S. Hossain, and M. Asif, "Dynamics of partially collapsing pulsed fluidized bed," *The Canadian Journal of Chemical Engineering*, vol. 99, no. 11, pp. 2333–2344, 2021.

[13] B. Leckner, "Fluidization characteristics of circulating fluidized bed boilers," *Chemie Ingenieur Technik*, vol. 95, no. 1–2, pp. 32–39, 2023.

[14] J. Zhu, H. Sun, W. Ren, X. He, L. Wang, Y. Yang, and G. Shi, "Emission characterization of particulate matters from the combustion of pulverized coals in a simulated fluidized bed boiler," *ACS Omega*, vol. 7, no. 42, pp. 37922–37932, 2022.

[15] Q. Lin, Y. Mei, W. Huang, B. Zhang, and K. Liu, "Understanding the role of polyvinylpyrrolidone on ultrafine low-rank coal flotation," *ACS Omega*, vol. 7, no. 12, pp. 10196–10204, 2022.

[16] H. Wu, T. Zhou, X. Hu, Y. Luo, M. Zhang, and H. Yang, "Thermal–hydraulic calculation and analysis on water wall system of a 700 MWe ultra-supercritical CFB boiler," *Energies*, vol. 16, no. 11, p. 4344, 2023.

[17] J. E. Galvin and S. Benyahia, "The effect of cohesive forces on the fluidization of aeratable powders," *AIChE Journal*, vol. 60, no. 2, pp. 473–484, 2014.

[18] J. C. Bandara, M. Sørflaten Eikeland, and B. M. E. Moldestad, "Analyzing the effects of particle density, size, size distribution and shape for minimum fluidization velocity with eulerian-lagrangian CFD simulation," in *Proceedings of the 58th Conference on Simulation and Modelling (SIMS 58), Reykjavik, Iceland, September 25th–27th, 2017*, vol. 138 of *Linköping Electronic Conference Proceedings*, pp. 60–65, Linköping University Electronic Press, 2017.

[19] T. Zhou, L. Qi, Y. Cao, G. Wu, and S. Li, "Study on the combustion and NOx emission characteristics of low rank coal in a circulating fluidized bed with post-combustion," *The Canadian Journal of Chemical Engineering*, vol. 95, no. 12, pp. 2333–2340, 2017.

[20] P. J. van Eyk, A. Kosminski, and P. J. Ashman, "Control of agglomeration and defluidization during fluidized-bed combustion of south australian low-rank coals," *Energy & Fuels*, vol. 26, no. 1, pp. 118–129, 2012.

[21] A. M. H. van der Veen, "Bayesian methods for type A evaluation of standard uncertainty," *Metrologia*, vol. 55, no. 5, pp. 670–684, 2018.

[22] V. Synek and S. Kříženecká, "Estimation of uncertainty from duplicate measurements: New quantification procedure in the case of concentration-dependent precision," *Accreditation and Quality Assurance*, vol. 28, no. 6, pp. 279–298, 2023.